# Microstructure Characterization of Weakly Textured and Fine Grained AZ61 Sheet

T.D. Berman[1], W. Donlon[1], C.K. Hung[1], P. Milligan[1], R. Decker[2], T.M. Pollock[3], J.W. Jones[1]

[1]Materials Science and Engineering, University of Michigan, 2300 Hayward St; Ann Arbor, MI, 48109, USA
[2]nanoMAG, LLC., 13753 Otterson Court; Livonia, MI, 48150, USA
[3]Materials Department, University of California, Santa Barbara; Santa Barbara, CA, 93106-5050, USA

Keywords: AZ61L, Microstructures, Texture, Mechanical Properties, Thixomolding, Thermomechanical Processing

## Abstract

Formability in magnesium alloy sheet is strongly limited by a strong basal texture in the as-rolled material, which is difficulty to remove by thermal processing. We introduce a new process to the control of texture by combining Thixomolding and Thermomechanical Processing (TTMP). Plates of AZ61L with a divorced $\beta$-$Mg_{17}Al_{12}$ eutectic are produced by Thixomolding, resulting in a non-textured, fine grained (2.8 $\mu m$) precursor. Sheet produced from the plate by single pass warm-rolling exhibits a weaker texture, and more isotropic tensile deformation than generally observed in AZ-series alloy sheet. Recrystallization annealing produces a further reduction in texture and average grain size (2.3 $\mu m$) and results in nearly isotropic room temperature deformation, a yield strength of $\sim$ 220 MPa, and an elongation of $\sim$ 23%. Particle stimulated nucleation of new grains by the $\beta$-phase during both dynamic and static recrystallization, is critical for achieving the low levels of texture. The influence of $\beta$-phase distribution in microstructure development is discussed.

## Introduction

Magnesium alloy sheet has many potential applications in reducing the weight of automotive, aerospace, and consumer electronics. However, the limited number of slip systems active at room temperature necessitate warm forming, which can make material costs prohibitive to widespread use. Several mechanisms have been employed to improve both the strength and formability of magnesium alloy sheet. Grain refinement is often employed to achieve a combination of high strength and high ductility [1]. Another important mechanism to improve ductility is texture control. Pronounced basal texture strongly reduces the formability of magnesium due to the inactivity of $\langle c+a \rangle$ slip [2]. It has been shown in weakly textured ECAPed material that the elongation to failure was over twice as high as that of the conventional AZ31 [3]. Stress-strain curves are orientation dependent in a textured material, and more isotropic behavior is produced from weaker textured material [4].

In order to produce fine-grained, weakly textured material a Thixomolded AZ61L plate was used as a precursor. As the dynamically recrystallized grain size depends on initial grain size in AZ series alloys [5], it is logical to start with the fine initial grain size from Thixomolding to produce sheet. Thixomolding also results in a distribution of relatively fine $\beta$-$Mg_{17}Al_{12}$ particles. The presence of these particles suggests opportunities to control the recrystallization texture and microstruc-

**Table 1:** Composition of received AZ61L in wt %

| Al | Zn | Mn | Si | Fe | Mg |
|------|------|------|------|-------|------|
| 6.5 | 0.46 | 0.14 | 0.01 | 0.003 | bal. |

ture by adjusting their size, distribution, and volume fraction [6]. Second phase particles can also suppress grain growth during hot working.

## Experimental

Preheated Thixomolded plates, with dimensions of 200 mm x 200 mm x 3 mm were preheated for 5 minutes at 315 °C and then warm-rolled in a single pass with a roll temperature near 200 °C. After rolling, the sheets were allowed to cool to room temperature in ambient air. The final sheet thickness was 1.8 mm, a thickness reduction of approximately 40%. Table 1 gives the composition of the AZ61L plates. Annealing treatments were done in a Techne SBL-2D fluidised bath. Annealed samples were water quenched.

Dogbone tensile specimens with a gauge length of 25.45 mm and cross section of 6.35 mm x 1.8 mm were machined from the sheets with the tensile axis (TA) at 0 °, 45 °, or 90 ° from the rolling direction (RD). Tensile tests were conducted at room temperature; samples were preloaded to 20 MPa and deformed at a displacement rate of 0.60 mm/min. At least three specimens were used for each condition. An extensonometer was

used to measure tensile elongation. Samples used for r-value measurements were strained to 10%.

All microstructures examine the plane of the sheet. SEM samples were prepared by polishing to 1 $\mu$m diamond paste followed by a chemical etch. The as-Thixomolded samples were etched for 10 s at room temperature in a 1:9 solution of o-phosphoric acid in ethanol. Wrought samples were etched for 5 s at room temperature in an solution of 10 ml water, 10 ml acetic acid, 4.3 grams of picric acid, and 70 ml of ethanol. SEM examination was conducted with a Philips XL30 FEG.

XRD pole figure analysis was conducted on the sheet cross section in order to be able to capture texture information that would fall at angles greater than 75° from the normal direction in the planar orientation. Specimen preparation involved polishing mounted cross sections to 1200 grit SiC paper with ethanol. A Rigaku rotating anode XRD system was used to make XRD pole figure measurements. XRD volume fractions were determined by using the whole pattern fitting routine in the Jade (2010) software package.

## Results

### Evolution of Mechanical Properties

Table 2 illustrates the evolution of mechanical properties as we go from the as-Thixomolded plate, to the as-rolled sheet, to sheet subjected to post-deformation annealing at 285°C for 10 minutes. The 3 mm thick molded plate has a mean ductility of 16% and a mean yield strength of 145 MPa.

The rolling process leads to a material twice as strong as the Thixomolded precursor. However, there is tensile anisotropy in the plane of the sheet; the ultimate tensile strength is ~25 MPa stronger along the RD than along the transverse direction (TD) (Figure 1). The average Lankford coefficient ($\bar{r}$) is 1.4 for the as-rolled sheet, with the planar anisotropy of r-value ($\Delta r$) being 0.3.

After annealing at 285°C for 10 minutes the yield strength of the sheet drops nearly 120 MPa to 225 MPa along the RD, however, the tensile deformation becomes much more isotropic in the plane of the sheet (Figure 1). In addition, the elongation along the RD increases to 24.7%. The improved isotropy is also evident in the Lankford values, with $\bar{r}$ being 1.09, and $\Delta r$ being 0.12 in the recrystallized sheet.

### Microstructures

Thixomolded Precursor The rapid solidification rate during Thixomolding results in a fine grain size and weak crystallographic texture. The microstructure is composed of fine $\alpha$-Mg grains surrounded by a divorced $\beta$ eutectic (Figure 2). The average grain size of the as-Thixomolded material, as measured near the surface of the sheet, is 2.8 $\mu$m. In addition to controlling the grain size, the rapid cooling rate leads to a supersaturation of aluminum; the average volume fraction of the $\beta$-phase is only 3% as determined by XRD and area fraction calculation. The $\beta$-particles are heterogeneously distributed throughout the microstructure, primarily along grain boundaries. The $\beta$-particles have a mean area of 31 nm with over 95% of the particles being less than 1 $\mu$m in area.

As-Rolled Sheet The as-rolled microstructure largely consists of heavily deformed grains. The $\beta$-phase network is elongated along the RD (Figure 3). The extended time at temperature during the rolling process leads to further precipitation of the $\beta$-phase. Due to

| Anneal | Angle | YS (MPa) | UTS (MPa) | Max Strain (%) | r | $\bar{r}$ | $\Delta r$ |
|---|---|---|---|---|---|---|---|
| as-Molded | 0 | 145.7 ± 6.4 | 272.8 ± 21.4 | 16.0 ± 6.5 | | | |
| as-Rolled | 0 | 344 ± 10 | 371.4 ± 4.1 | 14.6 ± 4.3 | 1.48 | | |
| | 45 | 271 ± 14 | 343.8 ± 5.1 | 16.7 ± 5.1 | 1.59 | | |
| | 90 | 260 ± 12 | 344.8 ± 1.1 | 15.0 ± 2.8 | 1.10 | | |
| | Mean | 292 | 353 | 15.4 | | 1.44 | 0.30 |
| 285°C | 0 | 225 ± 4 | 315.5 ± 0.3 | 24.7 ± 4.5 | 0.96 | | |
| | 45 | 212 ± 4 | 310.0 ± 2.5 | 26.1 ± 3.0 | 1.14 | | |
| | 90 | 219 ± 10 | 321.6 ± 8.9 | 19.0 ± 3.0 | 1.09 | | |
| | Mean | 219 | 316 | 23.3 | | 1.09 | 0.12 |

**Table 2:** Tensile properties of the Thixomolded plate and TTMP AZ61L sheet. The annealing treatment at 285°C was 10 minutes in duration. The angle is measured between the rolling and tensile directions. Samples strained to 10% were used for determination of the Lankford value.
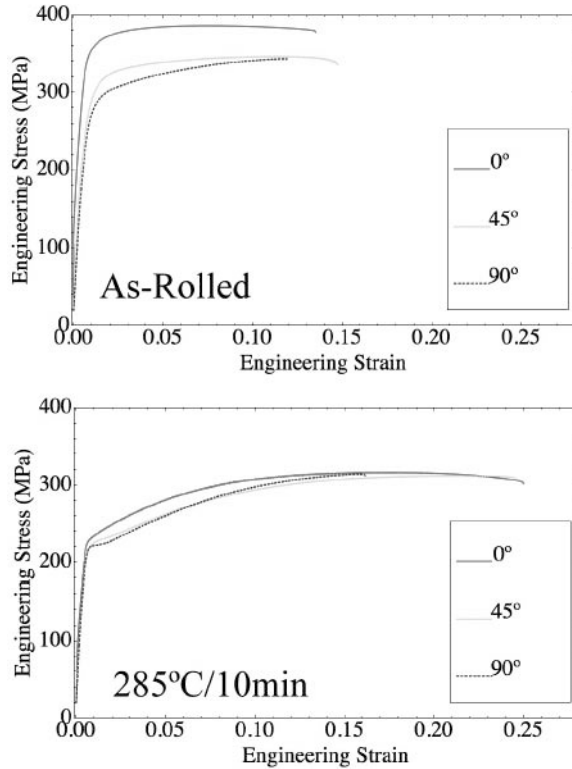
Figure 1: Engineering stress vs. engineering strain for as-rolled and annealed sheet.

a strong texture, it is difficult to measure the volume fraction of the $\beta$-phase via X-ray diffraction, however based on area fraction measurements of SEM images, the as-Rolled material has a $\beta$-phase volume fraction of 4.6%. $\beta$-particles in the as-rolled sheet can be classified into 2 groups, (1) large particles that existed in the as-Thixomolded microstructure and were deformed and coarsened during rolling and (2) fine spheroidal and rod-like particles that precipitated during rolling or during post-deformation cooling (Figure 4).

Annealed Sheet   Post-deformation annealing at 285 °C for 10 minutes leads to a fully recrystallized sheet the a average grain size of 2.3 $\mu$m (Figure 5). The grain size distribution is nearly identical to the original as-Thixomolded distribution (Figure 6). The $\beta$-phase network remains elongated in the RDs and the volume fraction of $\beta$ is nearly unchanged from the as-rolled condition at 4.8% as measured by XRD.

Deformed Sheet   Examination of one of the as-rolled tensile samples, which failed at 13% strain in the RD, reveals damage accumulation in the $\beta$-phase in the form of cracks and voids (Figure 7). The cracks run perpendicular to the TA and RD.
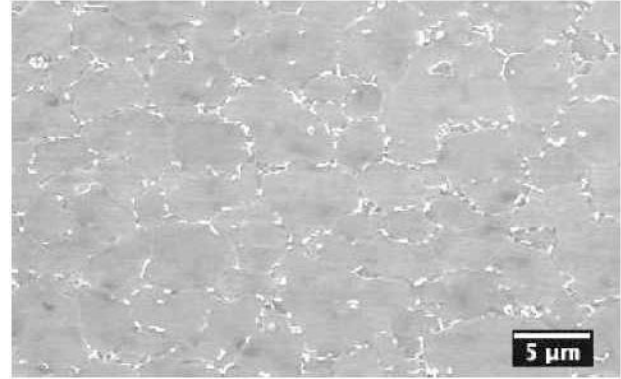


Figure 2: Microstructure of the as-Thixomolded plate. $\beta$-$Mg_{17}Al_{12}$, the brighter phase, forms a discontinuous network along the grain boundaries.
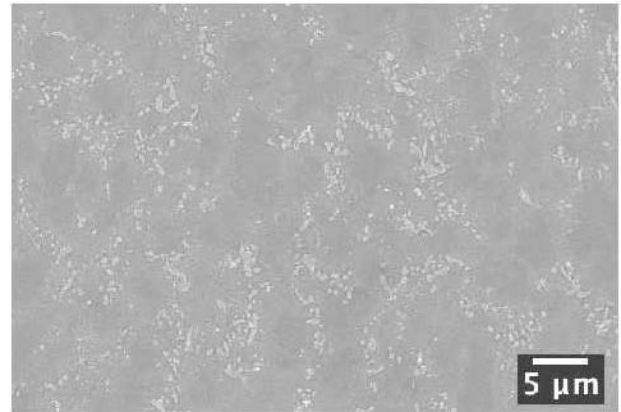


Figure 3: Microstructure of the as-rolled condition. The volume fraction of the $\beta$-$Mg_{17}Al_{12}$, has increased and the $\beta$-phase network is elongated in the RD (vertical).

Texture Evolution
The as-Thixomolded sheet has a near random intensity in both the 0002 and $10\bar{1}0$ pole figures (Figure 8). XRD pole figures reveal that the as-rolled sheet has a near basal texture in the plane of the sheet, with double averages located $\sim 20$ ° from the basal direction. The intensity of the basal texture is greatly diminished after annealing at 285 °C for 10 minutes. In addition, the peaks tilt further away from the basal pole, to near 45 °. The texture is elongated along the TD after rolling, as indicated by the $10\bar{1}0$ pole figures.

## Discussion

The texture of the rolled sheet is distinctive among AZ alloys. Figure 8 illustrates the weak (max = 3.1 times random), double-peaked basal texture. 10 times
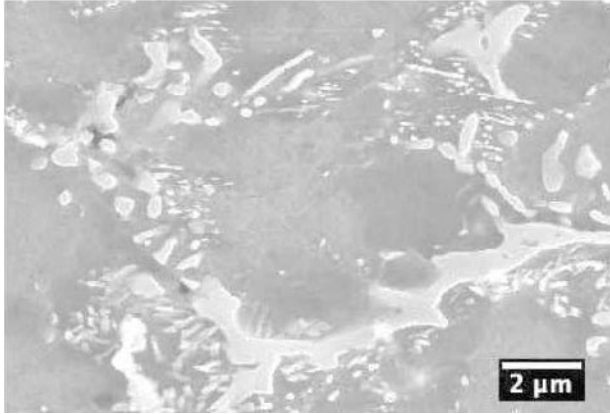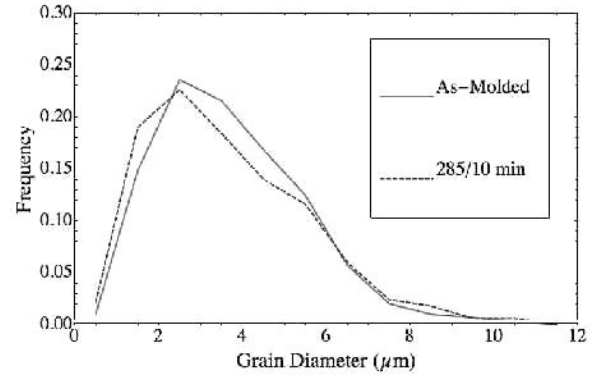
**Figure 4:** Microstructure of fine $\beta$-particles precipitated during the rolling process. Spherical and rod-like particles are evident.
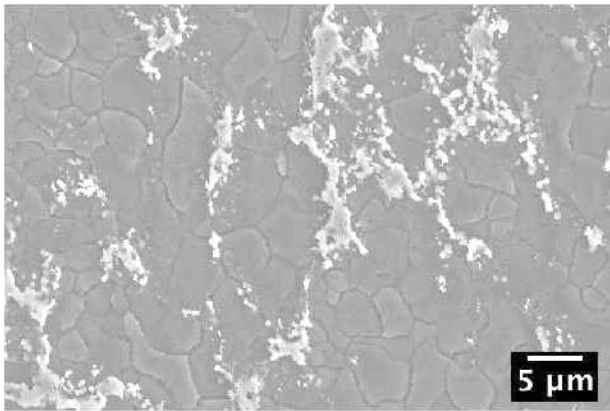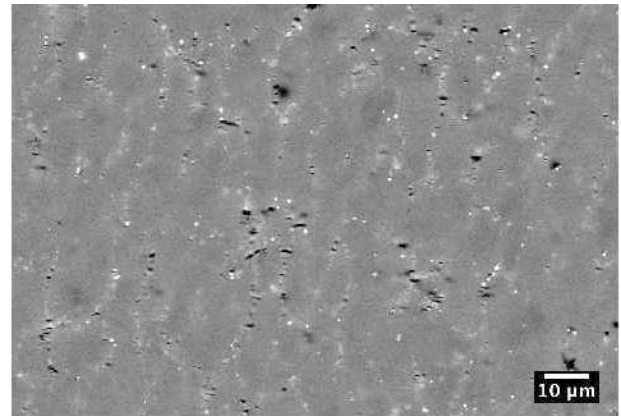


**Figure 5:** SEM microstructure of sample annealed for 10 minutes at 285 °C. The $\beta$-phase network remains elongated in the rolling (vertical) direction



**Figure 6:** Grain size distribution of the as-Molded and recrystallized (285C/10min) materials.



**Figure 7:** BSE image of damage accumulation in the as-rolled material when the TA is along the RD (vertical). It is clear that the damage is initiating in the $\beta$-phase.

random is typical for a basal pole figure intensity in the AZ series [7–11]. The peaks are tilted $\sim 20\,^\circ$ from the basal direction. A splitting, or elongation of the basal peak in the RD is commonly observed [7, 9, 12–15], this split likely results from increased activity of the $\langle c+a \rangle$ slip mode [16]. Li el al have shown that AZ61 and and AZ91 exhibit weaker texture after rolling due to particle stimulated nucleation [17]. The notable feature of the texture of TTMP AZ61L is that there is a preferential orientation of the $\langle 10\bar{1}0 \rangle$ directions, other reports on AZ series alloys that provide the $10\bar{1}0$ pole figure show a random orientation of **a** [7–9, 15]. Though not observed in AZ series alloys, textures similar to that of TTMP AZ61L, with a broader spread of the basal poles along the TD than in the RD, have been reported in RE containing wrought Mg sheets [18]. The mechanisms behind the development of the

RE textures are still not understood [19].

Another interesting feature of the texture of TTMP AZ61L is that it weakens during static annealing. Texture generally does not change during static annealing [4, 6]. Masoumi et al have shown texture reduction during the annealing of twin-roll cast AZ31, which they attributed to particle stimulate nucleation arising from a higher volume fraction of secondary phases [20]. This mechanism is likely active in the TTMP AZ61L sheet as well. Another postulate is that continuous recrystallization, which involves rotation of grains and subgrains, may become the dominate recrystallization mechanism in the TTMP AZ61L as pinning of grain boundaries and dislocations by $\beta$-particles hinders dynamic recrystallization. Similar observations have been made during dynamic recrystallization of RE alloys [21, 22]. Recrystallization occurring via lattice

116
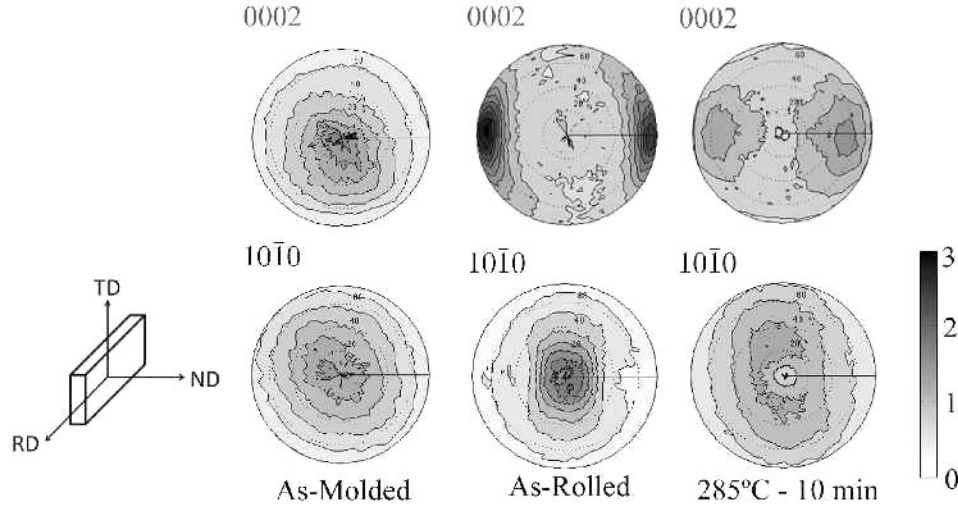
**Figure 8:** Measured pole figures for the material after molding, warm-rolling, and annealing at $285\,^{\circ}$C for 10 min.

rotations at grain boundaries can lead to a change in recrystallization texture [6].

The texture of the TTMP AZ61L leads to encouraging mechanical behavior. The average Lankford r-value $(\bar{r})$ is low for Mg-alloy sheet at 1.4. Average room temperature r-values in the range of 1.7 - 4.2 have been reported in AZ31 [7, 9, 10, 12, 13, 23]. Huang et al did measure low r-values (1.1 and 1.2) in AZ31 produced by multiple roll processing, with finishing passes at $525\,^{\circ}$C and $555\,^{\circ}$C [12]. Interestingly, in all of these studies, it was found the the r-value was higher in the TD than in the RD, whereas in the as-rolled TTMP AZ61L sheet the r-value was found to be higher in the RD than the TD. Similar observations have published on sheets of RE containing Mg-alloys and are a result of the unique textures exhibited by these materials [18]. Another mechanical property of the TTMP AZ61L that results from the RE-like texture is that the UTS of the material is higher in the RD than in the TD due to flow stresses being lower along the TD than in the RD.

A unique feature of the TTMP AZ61L is the $\beta$-phase network in the final sheet product. AZ-series alloys are usually solution treated, removing the brittle $\beta$-phase. Though the secondary phase provides for particle stimulated nucleation and grain size stability during annealing, it is clearly illustrated in Figure 7 that damage does initiate at either the $\alpha/\beta$ phase boundary or inside the $\beta$-particles. In both the as-rolled and recrystallized sheets we observed that the elongation is significantly lower along the TD. It has yet to be determined if this is due to the elongation of the $\beta$-phase network along the RD, which could allow for easier propagation of cracks perpendicular to the TA when the TD is parallel to the TA. Future work will be addressing the orientation dependence of damage accumulation in the TTMP AZ61 material at fixed strain increments.

## Summary

Warm-rolling of an AZ61L Thixomolded plate produces a Mg-alloy sheet with high strength and reasonable formability. The TTMP sheet exhibits a weaker texture, and more isotropic tensile deformation than generally observed in AZ-series alloy sheet. Annealing at $285\,^{\circ}$C for 10 minutes leads to a recrystallized sheet with a average grain size of 2.3 $\mu$m and an even weaker basal texture. These characteristics result in nearly isotropic room temperature tensile deformation, a yield strength of $\sim 220$ MPa and a elongation of $\sim 23\%$. The $\beta$-phase plays an important roll in both dynamic and static recrystallization, keeping the as-deformed texture weak and allowing for texture reduction during annealing.

## Acknowledgements

117

## References

1. J. Chapman and D. Wilson, "The Room-Temperature Ductility of Fine-Grain Magnesium," *Journal of the Institute of Metals*, 91 (1962), 39–40.

2. R. Gehrmann, M. Frommert, and G. Gottstein, "Texture effects on plastic deformation of magnesium," *Materials Science and Engineering A*, 395 (1-2) (2005), 338–349.

3. T. Mukai, "Ductility enhancement in AZ31 magnesium alloy by controlling its grain structure," *Scripta Materialia*, 45 (1) (2001), 89–94.

4. S. Agnew et al., "Enhanced ductility in strongly textured magnesium produced by equal channel angular processing," *Scripta Materialia*, 50 (3) (2004), 377–381.

5. H. Watanabe et al., "Grain Size Control of Commercial Wrought Mg-Al-Zn Alloys Utilizing Dynamic Recrystallization," *Materials Transactions*, 42 (7) (2001), 1200–1205.

6. F. Humphreys and M. Hatherly, *Recrystallization and Related Annealing Phenomena* (Elsevier, Netherlands, 2004), 2 ed.

7. S. Agnew and O. Duygulu, "Plastic anisotropy and the role of non-basal slip in magnesium alloy AZ31B," *International Journal of Plasticity*, 21 (6) (2005), 1161–1193.

8. A. Jain et al., "Grain size effects on the tensile properties and deformation mechanisms of a magnesium alloy, AZ31B, sheet," *Materials Science and Engineering: A*, 486 (1-2) (2008), 545–555.

9. S. Yi et al., "Mechanical anisotropy and deep drawing behaviour of AZ31 and ZE10 magnesium alloy sheets," *Acta Materialia*, 58 (2) (2010), 592–605.

10. Y. Chino, K. Sassa, and M. Mabuchi, "Enhanced stretch formability of Mn-free AZ31 Mg alloy rolled by cross-roll rolling," *Journal of Materials Science*, 44 (7) (2009), 1821–1827.

11. M. Masoumi, F. Zarandi, and M. Pekguleryuz, "Microstructure and texture studies on twin-roll cast AZ31 (Mg3wt.%Al1wt.%Zn) alloy and the effect of thermomechanical processing," *Materials Science and Engineering: A*, 528 (3) (2011), 1268–1279.

12. X. Huang et al., "Improvement of stretch formability of Mg3Al1Zn alloy sheet by high temperature rolling at finishing pass," *Journal of Alloys and Compounds*, 509 (28) (2011), 7579–7584.

13. H. Zhang et al., "Influence of initial texture on formability of AZ31B magnesium alloy sheets at different temperatures," *Journal of Materials Processing Technology*, 211 (10) (2011), 1575–1580.

14. L. Jin et al., "Effects of hot rolling processing on microstructures and mechanical properties of Mg3%Al1%Zn alloy sheet," *Materials Science and Engineering: A*, 527 (7-8) (2010), 1970–1974.

15. J. Koike, "Enhanced deformation mechanisms by anisotropic plasticity in polycrystalline Mg alloys at room temperature," *Metallurgical and Materials Transactions A*, 36 (7) (2005), 1689–1696.

16. S. Agnew, M. Yoo, and C. Tome, "Application of texture simulation to understanding mechanical behavior of Mg and solid solution alloys containing Li or Y," *Acta Materialia*, 49 (20) (2001), 4277–4289.

17. X. Li et al., "Influence of second-phase precipitates on the texture evolution of Mg Al Zn alloys during hot deformation," *Scripta Materialia*, 66 (2012), 159–162.

18. J. Bohlen et al., "The texture and anisotropy of magnesium zinc rare earth alloy sheets," *Acta Materialia*, 55 (2007), 2101–2112.

19. S. Agnew and J. Nie, "Preface to the viewpoint set on: The current state of magnesium alloy science and technology," *Scripta Materialia*, 63 (7) (2010), 671–673.

20. M. Masoumi, F. Zarandi, and M. Pekguleryuz, "Alleviation of basal texture in twin-roll cast Mg3Al1Zn alloy," *Scripta Materialia*, 62 (11) (2010), 823–826.

21. J. P. Hadorn et al., "Role of Solute in the Texture Modification During Hot Deformation of Mg-Rare Earth Alloys," *Metallurgical and Materials Transactions A*, 43 (April) (2012), 1347–1362.

22. K. Hantzsche et al., "Effect of rare earth additions on microstructure and texture development of magnesium alloy sheets," *Scripta Materialia*, 63 (7) (2010), 725–730.

23. M. Barnett et al., "Deformation mechanisms in Mg alloys and the challenge of extending room-temperature plasticity," *Jom*, 61 (8) (2009), 19–24.